RES MILITARIS
REVUE EUROPEENNE D ETUDES EUROPEAN JOURNAL OF MILITARY STUDIES
Social Science Journal

FORMULATION, OPTIMIZATION AND SOLUBILITY ENHANCEMENT OF GRISEOFULVIN USING BCYCLODEXTRIN AND PVPK30 AS TERNARY COMPLEX

[1]Ms. S. Harika, [2]Dr. K. Rajitha, [3]Mrs. D. Jyothi

[1]Assistant Professor, [2]Professor, [3]Assistant Professor

[123]Department Of Pharmaceutics

Vaagdevi Institute of Pharmaceutical Sciences, Bollikunta, Warangal. Telangana.

ABSTRACT

The goal of the current studies was to create a topical gel that contained griseofulvin's nanostructured lipid carriers (NLCs) and evaluate how well it worked for superficial infections. Using a variety of lipids and surfactants, including oleic acid, glyceryl monostearate, pluronic F 68, and tween 80, the drug solubility tests were carried out. Box-Behnken design (BBD) was used to optimize the lipid, surfactant, and emulsifier concentrations. Superosonication was used to create microemulsions. The optimized batch (F12), which contained 0.2% w/w drug, 2% GMS, 2% Pluronic F68, and Tween 80 (in a 1:1 ratio) showed a particle size of 209 nm, a zeta potential of -44.12 mV, an entrapment level of 85.24%, and a drug release of 92.12% after the prepared batches (F1 to F15) were analyzed. The topical gel was made with 1.5% carbopol 940. Biochemical investigations showed that, in comparison to the typical medication, griseofulvin-loaded nanogel significantly reduced lipid peroxidation. Studies on the cytotoxicity of nanogel in vitro revealed increased safety for human keratinocyte cells (HaCaT). Using T.rubrum and M.canis fungal strains, the findings of antifungal activity demonstrated complete clinical and mycological cure against superficial infections including Tenia pedis as well as ringworm in Wistar rats in a period of 21 days. These preclinical studies have demonstrated that nanogels are a more promising treatment option than currently available medications for the aforementioned superficial infection

Introduction

Fungi are the most common microbial agents responsible for the prevalence of skin diseases globally. Pathogenic fungi dwell in hair, nails, epidermis, and mucosa causing superficial fungal infections. The three most common superficial infections are Dermatophytosis (tinea or ringworm), Pityriasis versicolor, and Candidiasis (Kelly, 2012). Dermatophytosis has become more common in recent decades with an estimated incidence of 25% of the global population (Teklebirhan & Bitew, 2015) representing the third most common fungal illness globally (Rouzaud et al., 2017). Trichophyton spp., particularly Trichophyton, Microsporum, and Epidermophyton are the major agents accountable for skin infections.

There are several antifungal medications that are previously generated and proven themselves to be effective in killing the superficial fungi, but they have failed in providing the required therapeutic effect due to their poor aqueous solubility and permeability. As a result, fresh and more

advanced antifungal therapeutic alternatives are desperately needed (Arnold et al., 2010). Griseofulvin is a heterocyclic benzofuran found in the Penicillium. It belongs to BCS class II medication ith a log P value of 2.17 and shows high permeability and low solubility (Arida et al., 2007). A study revealed that despite all the favorable molecular features such as lipophilicity, molecular mass (352.77 Da), and hydrogen bond accepting capacity (Veber et al., 2002) topical dosage for griseofulvin is not so promising due to limitations of solubility and penetrability to the deeper layers of the skin.

Topical management of fungal infections has various benefits like fewer side effects, site-specific administration, high patient compliance, and effective cure. Antifungal treatment tactics have become increasingly complex and expensive due to a lack of effective medications and a rising proportion of drug resistance. There have been a lot of recent findings on topical formulations of griseofulvin to increase penetration through skin by dissolving the agent in a variety of vehicles (Aggarwal & Goindi, 2012), use of new carrier systems (Pierri & Avgoustakis, 2005), and more recently, by using penetration enhancers (Fujii et al., 2000). The topical delivery of antifungal agents into the skin is improved by new drug delivery technologies such as vesicular carriers, colloidal systems, and nanoparticles (Lee & Maibach, 2006). There are some recent findings where researchers explored the potential of griseofulvin in colloidal carriers viz polylactide micelles (Pierri & Avgoustakis, 2005) nanoparticles (Kamiya et al., 2010) deformable membrane vesicle (Aggarwal & Goindi, 2012), ethosomes (Aggarwal & Goindi, 2013) (Marto et al., 2016) and liposomes (Bavarsad et al., 2016). Nanostructured lipid carriers (NLCs) are made up of a mixture of solid & liquid lipids. They can integrate large amounts of pharmaceuticals into this sort of carrier/delivery system due to the production of a less structured lipid matrix with several defects (Gaba et al., 2015), (Firooz et al., 2015). The NLCs containing antifungal gel were chosen above other colloidal components such as SLN, liposomes, and nanoparticles because of their ease of manufacture, high drug loading capacity, and better stability (Vicentini et al., 2011). Thus, the present study was started with the goal to develop griseofulvi.

Experimental

2.1. Material and methods

Griseofulvin was procured as a gift sample from Wallace Pharmaceuticals Ltd., Mumbai, India. Tween 80, sodium hydroxide pellets were purchased from S D Fine-chem Limited, Mumbai. Methanol was procured from Chong Yu Hi-Tech Chemicals China and poloxamer 188(Pluronic F68) from Hi-Media Pvt Ltd. Glyceryl monostearate was purchased from Tokyo Chemicals, thiobarbituric acid from Molychem, Mumbai, oleic acid from Thomas Baker Chemicals Ltd, Mumbai. Triple distilled water (TDW) was used throughout the study. The rest of the reagents and chemicals were analytical grade & used without additional processing.

2.2. Solubility screening of lipids and surfactant

Glyceryl monostearate, oleic acid, Pluronic F68, soya lecithin, and castor oil were used to evaluate the solubility of the drug, griseofulvin. For this, an excess quantity of the drug was administered to the vial

containing the screening sample, closed the vial, and agitated for 12 12 hours at 37 ± 2 degrees Celsius in a wrist shaker bath. The dispersion was centrifuged for 10 min at 10,000 rpm, and the resulting supernatant was mixed with the suitable lipids, filtered, and evaluated using a UV spectrophotometer (UV-1700, Shimadzu, Japan) (Mahmood et al., 2018).

2.3. Screening of solid and liquid lipids for solubilisation of drug

Various solid and liquid lipids were tested for the level of solubility of the drug in them. The procedure of the test included the addition of 100 mg of the drug to 5 g of solid lipid followed by heating till the lipid melted. In the case of liquid lipids, 100 mg of drug was added to 5mL of liquid lipid and visually tested for any occurrence of crystals. After the transparency was achieved drug was added further till the concentration of the preparation became 0.2% w/v in the formulation (Mura et al., 2021).

2.4. Optimization of process parameters and formulation

Box-Behnken design was used to the optimized NLCs of Griseofulvin. To optimize, the amount of the solid lipid, Glyceryl monostearate (X1), Oleic acid (X2), and sonication time (X3) were selected as independent variables. Every factor was set at the high medium and low levels. The real and coded values of different variables are given in Table 1. The particles size, entrapment efficiency, and cumulative release were taken as dependent variables (Pal et al., 2019).

2.5. Formulation of NLCs

The Griseofulvin-loaded-NLCs dispersion was prepared by emulsion solvent diffusion and evaporation method, followed by ultrasonication.

Table 1 Variables in Box-Behnken design for formulation of griseofulvin-loadedNLCs.

Variables	Levels		
Independent variables	**Low**	**Medium**	**High**
X1 = GMS: Stearic acid	1:25	1:50	1:01
X2 = Pluronic F68: Tween 80	1:1	1:1.5	1:2
X3 = Sonication time (min)	45	60	75
X4: Oleic acid (v/v)	1.0%	1.5%	2.0%
Dependent variables			***Constraints***
Y1 = Particle size (nm)			Minimize
Y2= Entrapment efficiency (%)			Maximize

A mixture of glyceryl monostearate and oleic acid (1-2%) was melted together. Simultaneously, a transparent drug solution was prepared by adding griseofulvin (0.2% w/w) to a mixture of acetone (2 mL) and methanol (3 mL) at 60 ˚C in a water bath and then incorporated with the melted lipid solution. The rest of the procedure was followed as done by (Waghule et al., 2020).

2.6. Characterization

2.6.1. Particle size, polydispersity index and zeta potential

Malvern Zeta-sizer TM was used to evaluate the vesicle size, distribution profile, and zeta potential of the optimized NLCs gel. To eliminate multiple scattering effects, the vesicle solution was adequately reduced using pure water for the vesicle size measurements. The range of the size distribution was measured using the polydispersity index (PDI). The solution was diluted with filtered water to adjust the conductivity to 50 mS/cm in a zeta cuvette, and then zeta potential was determined.

2.6.2. Morphology and shape

The surface morphology of the optimized batch of griseofulvin-NLCs was investigated using a scanning electron microscope (SEM) (JEOLJSM-6490LV,

Japan). NLC dispersion was mounted on aluminium stubs, further coated with gold by a vacuum evaporator, observed, and photographed.

2.6.3. Entrapment efficiency (EE)

Nanogel was liquefied insolvent using a magnetic stirrer for 30 min. The resultant dispersion was centrifuged (3-18 K, Sigma) at 10,000 rpm for 10 min and the drug content present in the supernatant was analyzed at λmax 293 nm using UV spectroscopy (UV-1700, Shimadzu, Japan). The entrapment efficiency was calculated using under mentioned equation (Hu et al., 2006).

$$EE\ (\%) = \frac{\text{Weight of drug in nanogel} - \text{Free drug}}{\text{Weight of drug in nanogel}} * 100 \quad (1)$$

2.6.4. Incorporation of NLCs dispersion in gelling agent

Griseofulvin-loaded-nanogel was prepared by varying the concentrations of Carbopol 940 (0.5%, 1.0%, 1.5%, and 2.0% w/v) among which 1.5% was chosen as optimized one because of its good physical properties and more cumulative percutaneous drug accumulation by topical route. The desired amount of Carbopol 940 was dispersed in purified water with the addition of 5% v/v glycerol for increasing hydration. Other methods were carried out as expressed by (Rajinikanth & Chellian, 2016).

2.6.5. Rheology (Viscosity)

The viscosity of the gel was measured by Brookfield viscometer (Model-RV) at 25 ˚C. The gel was taken in a beaker and spindle number 7 was dipped in the gel. Four readings were recorded at 10, 20, 50, and 100 rpm. The dial reading was noted and viscosity was calculated by the equation (Joshi & Patravale, 2006).

$$\eta(\text{Centipoise}) = \text{Factor} * \text{dial reading} \quad (2)$$

2.6.6. Chemical Characteristics (FT-IR)

Chemical characterization of Griseofulvin, PEG 6000 and microwave irradiated solid dispersion in terms of functional group, structure, and interaction b/w drug & polymer was evaluated by an FT-IR spectrophotometer (FT-IR Bruker). FT-IR spectra were obtained in the range of 400-4000 cm−1 at BBDNIIT, Lucknow (Sarfraz et al., 2019).

2.6.7. In-vitro drug release

Franz diffusion cell was used for the in-vitro drug release study with Phosphate buffer solution of pH of 7.4 in the receptor compartment and 0.5 gm prepared gel in the donor compartment. The gel was mixed using a magnetic stirrer and the temperature was maintained at 37 ˚C. The sample was withdrawn at regular intervals, and the sink condition was maintained with phosphate buffer solution. UV spectroscopy was used to analyze the samples at 293nm (Sanad et al., 2010, Chen et al., 2012).

2.6.8. Ex vivo permeation study

Ex vivo investigations on mice skin were performed using phosphate buffer solution in the receptor compartment (pH 7.4). The skin was extended over a Franz diffusion cell at 37˚C for 1 hour. At certain intervals, a volume of 1 mL of solution was withdrawn and a sample was withdrawn and replaced with the same level of buffer solution as performed by Asad et al. (2021).

2.6.9. HET-CAM Study (Hen's egg test-chorioallantoic membrane)

Eggs were incubated for 9 days at 37±0.5 ˚C temperature and 62±7.5% relative

humidity. On day 10, the eggshell was cracked and removed. About 1 cm2 of the test sample was carefully placed directly upon CAM for 300 seconds and reaction time was recorded. After that 0.1 M NaOH as (+) ve control and 0.9% NaCl as (-) ve control was selected. Photographs were captured before and after the application of the formulation. Irritancy was calculated in terms of irritation score (IS) using the given equation (Lima et al., 2016, Harnoss et al., 2019, Lorenzo Veiga, 2020).

$$\text{Irritation score (IS)} = \frac{301 - t(h)}{300} * 5 + \frac{301 - t(l)}{300} * 7 + \frac{300 - t(c)}{300} * 9 \quad (3)$$

Where, h is haemorrhage, l is lysis, c is coagulation and t is time in seconds.

2.7. Pharmacological study

2.7.1. Fungal strains

The standard strains of dermatophytes, Trichophyton rubrum (MTCC 296), M. canis (MTCC no.2820), were procured from Microbial Type Culture Collection (MTCC), IMTEC Chandigarh, India.

2.7.2. Study animal

Experimental animals, male Wistar rats (9–10 weeks old) were procured from Faculty of Pharmacy, Babu Banarsi Das Northern India Institute of Technology, Lucknow, India. The study animals were kept in polypropylene enclosures and employed in ex-vivo permeation as well as in-vivo studies. Rats were housed at room temperature with a 12- hour night/day cycle and given a regular pellet meal and free access to water. The protocols for animal use and care were approved by the Institutional Animal Ethics Committee (IAEC), BBDNIIT, Lucknow, India (BBDNIIT/IAEC/2020/08).

2.7.3. Pharmacodynamic evaluation using T. rubrum and M. canis induced Tinea pedis and ringworm infection

The anti-fungal activity of the optimized griseofulvin-loaded-NLCs gel was assessed against Tinea pedis and ringworm infections. T. rubrum and M. canis strains were selected to induce the infections (Shimamura et al., 2012). A comparative study was performed to access the effectiveness of prepared nanogel taking control, test (nanogel), and standard drugs (marketed product) in the groups of 5 animals.

3. Results and discussion

3.1. Formulation development

3.1.1. Selection of solid lipid, liquid lipid, and surfactant

3.1.1.1. Selection of solid lipid, liquid lipid, and surfactant.

The solubility of the drug in various lipids and surfactants is crucial for selecting additives for the formulation development as it highly influences the solubility of the drug in the oil phase. The highest solubility of griseofulvin was reported in Glyceryl monostearate (4.5 mg/mL) followed by other lipids and surfactants as shown in Fig. 1. Therefore, glyceryl monostearate, oleic acid, Pluronic F68, and tween 80 were chosen for NLC preparation (Gaba et al., 2015; Beg et al., 2012). Soluble testing of Griseofulvin in solid and liquid lipids is considered important as it is a critical condition for obtaining good drug loading in the prepared composition. Once the clear solution was obtained, another 100 mg of the drug was added, to achieve a target concentration of 0.2% w / v in the final formulation. In all solid lipids, liquid lipids, and surfactants, glyceryl monostearate and

a combination of stearic acid as solid lipid and oleic acid as a liquid lipid accompanied by surfactant and co-surfactant (Poloxamer 188 and Twee-80) were selected as the best combination based on transparency (Mura et al., 2021).

3.2. Optimization of process parameters for NLCs

The optimization of process parameters for the development of NLCs containing gel was done by the Box-Behnken Design method. A total of 15 confirmatory runs with 3 center points were developed by having 3 independent and 2 dependent variables. Based on the preliminary screening of solid lipid ratio (%, X1), surfactant ratio (%, X2), time of sonication (X3), and liquid lipid (X4) values were selected and set at three levels low (-), medium (0), and high (+), as shown in Table 1. All developed formulations were subjected to characterizations like particle size, polydispersity index, zeta potential,%age drug entrapment, and in vitro release. The advantage of the BBD model was that the design usually had fewer design points, hence they were often less expensive to run than the CCD design with the same number of independent variables (Moghddam et al., 2016).

These independent elements were calculated based on the two dependent variables, particle size (nm Y1) and entrapment efficiency (%, Y2). 15 different batches were attained by altering the levels of lipids added designated as low, medium, and high, amounts of surfactant added, and the sonication time. The connection between independent parameters and the particle size, zeta potential, Polydispersity index (PDI), and entrapment efficiency was established (Moghddam et al., 2017). The optimized formulation (F12) showed a particle size of 209.7 nm, PDI of 0.237, and entrapment efficiency of approximately 85%. The zeta potential of the formulation was found to be negative (-44.12 mV), which can be ascribed to the lipids' negative charge indicating the stability of the nanocarrier as shown in Fig. 2. It is considered that the zeta potential values above ± 30 mV are found to be a good indicator of the stability of suspended particles (Uprit et al., 2013). Lipid nanoparticles exhibit stability problems but yet scientists have produced results with stability sustained with lyophilization and also by attaining a zeta potential of more than 30 mv (Yadav et al., 2013, Kovačević et al., 2014). A high value of negative or positive potential on all the particles will result in the repulsion of particles, hence reducing the possibility of aggregation (Khosa et al., 2018). It was also observed that formulae with higher content of oleic acid in the griseofulvin–NLCs resulted in higher zeta potential values and vice versa. This was attributed to the presence of the carboxylic (COO–) group in the oleic acid (Teeranachaideekul et al., 2007). Another study of isotretinoin-loaded SLNs preparation by (Liu et al., 2007) demonstrated that particle size was found to decrease with an increase in surfactant concentration (Das et al., 2011). This could be ascribed to the higher concentration of surfactant which effectively covers the surface of the lipid phase, resulting in the particle size reduction (Helgason et al., 2009). Furthermore, hydrophilic coating of tween 80 could also improve the lipid stability present in NLC, by hydration of the surface layer (Teeranachaideekul et al., 2007, Das et al., 2011).

3.3. Effect of independent variables on particle size, entrapment efficiency

Particle size has a huge influence on the level of drug absorption. The relationship between drug absorption and particle size is inversely proportional (Teeranachaideekul et al., 2007, Das et al., 2011). The particle size was found to decrease with an increase in the sonication time and increase in the concentration of surfactant as the surfactant will be forming a thick protective layer preventing the smaller droplets from aggregating. Sonication is done at ultrasonic amplitude to prevent the formation of large droplets (Kaur et al., 2014). Similarly, sonication time also has a great influence on the droplet size and poly dispersibility index in an inversely proportional way. Entrapment efficiency also is considered an important parameter as its understanding prevents the wastage of the drug (Singh et al., 2021).

The entrapment efficiency of the optimized batch, F12 was found to be 85.24%. During the optimization process, good entrapment efficiency was achieved starting from 37% to 89% as shown in Fig. 6. From the results obtained it was found that an increase in the concentration of oleic acid and sonication time increased the entrapping capacity. Griseofulvin-NLCs showed a drug content of 90.12 ± 4.6% w/v. It was also noticed that on increasing the lipid portion relative to the drug, the amount of drug entrapped into the lipid matrix and hence entrapment efficiency increased significantly. However, on an increasing amount of liquid lipids, the solubility of drugs and hence, the efficiency of drug entrapment increased comprehensively (Thakkar et al., 2014)

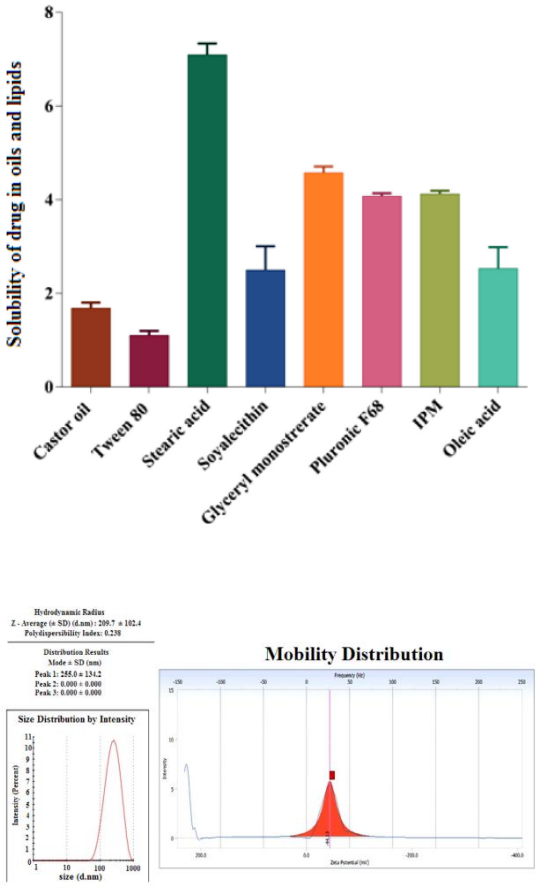

Fig. 2. Image of optimized batch of NLCs (F12) obtained for particle size, zeta potential and PDI.

3.4. FTIR

The FTIR studies showed significant peaks of griseofulvin with peaks due to C–N stretching at 1444.02 cm−1, C=O vibration at 1682.16 cm−1, and C–O–C at 1085.35 cm−1, N–H at 3301.77 cm−1, C=C group vibration at 1630.68 cm−1 and O–H vibration at 2799.45 cm−1 (Fig. 4a). The functional group peaks were coinciding with standard griseofulvin pure drug. IR analysis showed Griseofulvin has the first peak at 1712 cm−1 corresponding to the stretching of the carbonyl group of the benzofuran region and the second peak at 1662 cm−1 corresponding to the stretching

of the carbonyl group of cyclohexane. In context, the pure Griseofulvin exhibited clear peaks characteristic of the Griseofulvin at 3436, 2944, 1712, 1615, and 1584 cm−1 indicating adsorbed water vapor from the environment, vibrations in CH2 groups, the C=O stretch of the benzofuranone ring, cyclohexanone carbonyl hydrogen bonds and C=C stretch of the cyclic ring, respectively. The IR spectra of Glyceryl monostearate showed characteristic absorption band at 3308.85 cm−1, 2914.66 cm−1, 1729.99 cm−1, 1215.11 cm−1, and 1393.83 cm−1 which represent the presence of broad, O–H stretching vibrations, C–H stretching, C–O stretching of carboxylic acid, and C–O stretching vibration of tertiary alcohol, indicating no changes in functional groups (Al-Zein et al., 2011). The IR spectrum of poloxamer 188 (Fig. 4c) is characterized by principal absorption peaks at 2881.4 cm−1 (C–H stretch aliphatic), 1456.8 cm−1 (CH3 bend), and 1279.2 cm−1 (C–O stretch), which were consistent in all binary systems with the drug. The FTIR of Nanogel (Fig. 6 d) showed characteristic peaks of Griseofulvin, demonstrating the presence of the drug without any interaction. FTIR spectra of Oleic acid were characterized by the presence of a characteristic peak at 2926 cm−1 (C–H stretching) 1710 cm−1 (C=O stretch) and 1462 cm−1 (O–H bend) as shown in (Fig. 6e) (Cortés et al., 2012).

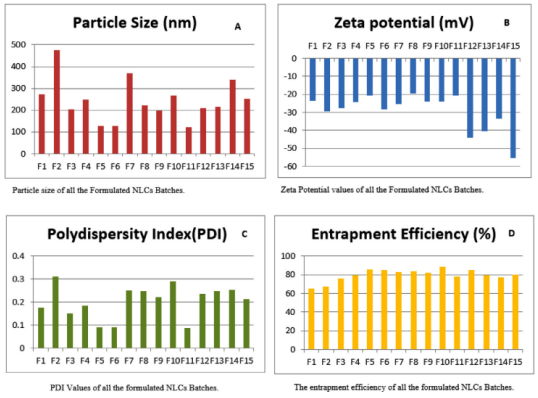

Fig. 3. Physicochemical Properties of Griseofulvin NLCs in terms of Particle side, Zeta Potential, Polydispersity index (PDI) and Entrapment efficiency. (n = 3, mean ± standard deviation (SD)).

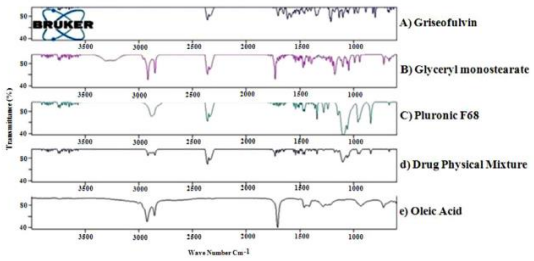

Fig. 4. FTIR of (A) Griseofulvin (B) Glyceryl monostearate (C)Pluronic F68 (D) Griseofulvin + Pluronic F68 + Glyceryl monostearate + Stearic acid + Carbopol940(E) Oleic acid.

3.5. Morphology and shape characterization

Scanning electron microscopic (SEM) analysis was performed to collect more information about particles and their size. Images showed the presence of spherical particles in the nanometer size range without any crystal particles as shown in Fig. 5. Aggregation of particles was also observed due to the lipid nature of carriers and sample preparation before SEM analysis. The formation of degenerative particles may be due to lipid modification during the drying of the sample treatment (Uprit et al., 2013).

3.6. Optimization of Gelling agent and Rheological behaviour of Nanogel

Different concentrations of the gelling agent Carbopol 940 were formulated and characterized for various parameters like spreadability, extrudability, and rheology, and based on these values the concentration of 1.5% was selected as the best due to its good physical properties and more

cumulative percutaneous drug accumulation by topical route (Rahmawati and Setiawan, 2019). This might be due to the solid elastic behavior of polymer due to more entanglement between polymer networks. Rheological characterization of optimized NLC dis

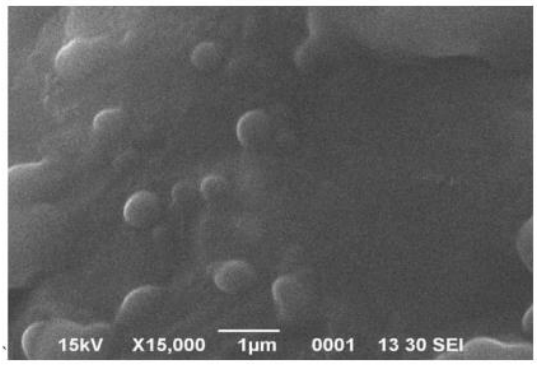

Fig. 5. SEM image of NLCs (Optimised 12).

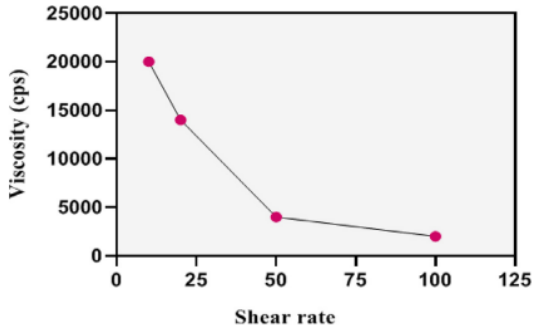

Fig. 6. The impact of shear on Rheology of NLCs containing Nanogel.

persion incorporated in the gel was done to observe the effect of the increasing rate of shear on the gelling agent. The impact of shear (rising) on the viscosity of nanogel is depicted in Fig. 6. As the shear rate was increased, the viscosity of nanogel was reduced, which suggested its pseudo-plastic nature owing to loss of compact packing and disruption of the inter-droplet network for attractive and repulsive nanogels, respectively (Rajinikanth et al., 2016).

3.7. In vitro drug release In-vitro drug release

study values ranged between 50% and 92.24%. The drug-loaded NLCs of griseofulvin as shown in Fig. 7a. The initial rapid in-vitro drug release might be due to surface release followed by a slow release from the solid lipid core of NLCs. The release profile of the optimized NLC, dispersion, and topical marketed product of investigated drug were studied comparatively as represented in Fig. 7b and was observed that there was a relatively faster release than the NLC gel and marketed formulation. The drug release from NLCs loaded topical gel was higher (80 ± 0.87%) and faster than that of commercial cream (50.2 ± 0.69%) which might be due to the involvement of oils that enhance the solubilization, and drug release. There was an initial burst release noted which might be attributed to entrapment of griseofulvin superficially as a result of sudden cooling from high temperature. There was a significant difference observed between the variables since the P-value ($P < 0.0001$) in the ANOVA was at the 99% confidence level.

To the data obtained from in-vitro drug release studies, various kinetic models were fitted. The kinetic model for F12 formulation was considered the best based on the R2 value which was found to be 0.9805 for the Korsmeyer–Peppas, with the descending values for first-order as 0.9189 followed by Higuchi matrix with an R2 value of 0.8815 and then finally zero-order with an R2 value of 0.7043 (Gouda et al., 2017).

3.8. Ex-vivo permeation study

The in-vitro permeation study was conducted using a Franz diffusion cell

along with an egg membrane and the results were acquired as represented in Figure 7c. The increased drug permeation from nanogel might be due to its nanosize, and the positive influence of surfactant and lipids. In the comparative study of drugs permeated from the NLCs and commercial products, the increased%age of drug release with a value of 50% as compared to29% from the commercial might be a result of decreased particle size, enhanced lipid friendliness. The permeation of the drug through the skin is slow and retention in the skin is for a longer time (Mahdi et al., 2021). The solubility and permeation both were higher with an increase in surfactant concentration which might be the release of the drug from the outer shell and increased partitioning of the drug between the melted lipid phase and the aqueous surfactant phase (Zur Mühlen et al., 1998). Oleic acid acts as a permeation enhancer with modification of SC lipids, thus, creating a new type of lipid base that can reduce the potency of the skin barrier. Therefore, it will disrupt and increase lipid packing and reduces resistance, helping in penetration. After applying statistical parameters, a significant difference was observed between the variables, Since the P-value ($P < 0.0001$) in the ANOVA was at the 99% confidence level (Mahmoud et al., 2020).

3.9. Differential scanning calorimetry (DSC)

The Thermogram of pure griseofulvin in Fig 8(a) revealed strong peaks at 219.44 ˚C. Omar et al. (2020) suggesting the drug's crystalline form with onset at 216.94 ˚C and ending at 221.9 ˚C, having enthalpy fusion energy ΔH of 112.43 J/ g. The glass transition temperature was found to be 30.65˚C (Vasa et al., 2014). The endothermic peak of the GMS in the DSC curve in Fig 8(b) was detected at about 58°C representing the melting temperature of GMS. The results were in good agreement with the reported melting endothermic maxima of GMS between 56.5 ˚C and 62.5 ˚C (Ding et al., 2018). However, the thermogram of griseofulvin-loaded topical nanogel in Fig 8 (c) depicted that in contrast to the pure griseofulvin, there was a significant drop in endothermic peak elevations and heat of fusion, indicating a transition from crystalline to amorphous state in nanogel, with a wider peak at 89.83 ˚C, and enthalpy fusion energy ΔH of 1594.51 J/g. Similar findings were obtained by (Kassem et al., 2017) suggesting the conversion of the crystalline drug to its amorphous state. This signified the possibility of interaction between the drug and the lipid responsible for better solubility of the drug which in turn affects its release from the nanoparticles (Omar et al., 2020).

3.10. Hen's egg chorioallantoic membrane test (HET-CAM) for skin irritation

The HET-CAM assay was used to examine the vascular irritation and biocompatibility of the griseofulvin-loaded nanogel, and the findings are given in Fig 9. After exposure, no signs of hemorrhage, lysis, or coagulation were observed in the griseofulvin-loaded nanogel (test formulation) or 0.9% NaCl (-ve) control, in contrast to the 0.1M NaOH (+ve control) which caused adverse outcomes such as bleeding, lysis, and coagulation. The irritation score for griseofulvin-loaded nanogel with 0.9% NaCl was found to be 0.069, whereas the score for 0.1m NaOH was found to be 15.23. Therefore, griseofulvin-loaded nanogel was found to be non-irritant and biocompatible in the

HET-CAM assay (Sandeep, 2020), Lima et al., 2016, Harnoss et al., 2019, Lorenzo Veiga, 2020).

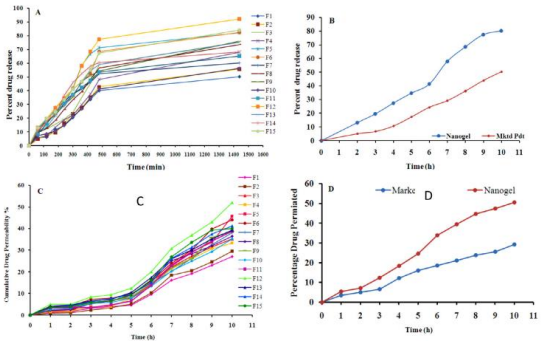

Fig. 7. (a) Cumulative in vitro drug release study of Griseofulvin loaded NLCs.

(b) Comparative In vitro Drug Release study Griseofulvin Nanogel with Marketed Product.

(c) Ex-vivo permeation study Griseofulvin loaded Nanogel.

(d) Comparative Ex-vivo permeation study Griseofulvin Nanogel with Marketed Product. ((n = 3, mean ± standard deviation (SD).

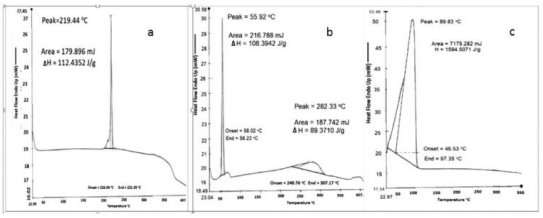

Fig. 8. DSC thermogram of pure Griseofulvin drug (a), Glyceryl monostearate (b), and Griseofulvin-loaded topical nanogel (c).

3.11. Animal studies

3.11.1. Histopathology of ringworm and Tenia pedis infection

3.1. Histopathology of ringworm and Tenia pedis infection.

Histopathological analysis of rat skin for Tenia pedis and ringworm was performed by using control, standard, and test (nanogel) formulations and observed for any morphological changes after treatment. Epidermal erosion (indicated by red arrow) and dermal edema (yellow arrow) in H and E Stain at 100X (A) and 400X (B) were observed as shown in Fig 10 (Control 1 – for Ringworm infection). Similarly, Fig 11 showed dermatitis characterized by infiltration of inflammatory cells in the dermis, epidermal erosion of Control 2 – for Tenia pedis infection, arrowheads representing dermatitis. This is characterized by infiltration of inflammatory cells in the dermis and some disruptions of the stratum corneum layer with an increased intercellular gap at a magnification of H&E Stain 100X (A) and Stain 400X (B). In Fig 12 the effect of nanogel (Test1) on ringworm was observed with the regeneration of normal epidermis (E), dermis (D), and subcutis, (Green arrow) at 100 and 400X H and E Stain. Similar results were observed after the application of nanogel on Tenia pedis-infected rats (T2) as shown in Fig 13 representing regeneration of hair follicles (Black arrow) of the normal epidermis (E), dermis (D) at 100 and 400X magnification. Marketed products also showed similar results but took more time and dosing frequency with lesser cell regeneration ratio of the normal epidermis (E) and dermis development (D) along with epidermal hyperplasia (Blue arrow) as shown in Fig 14.

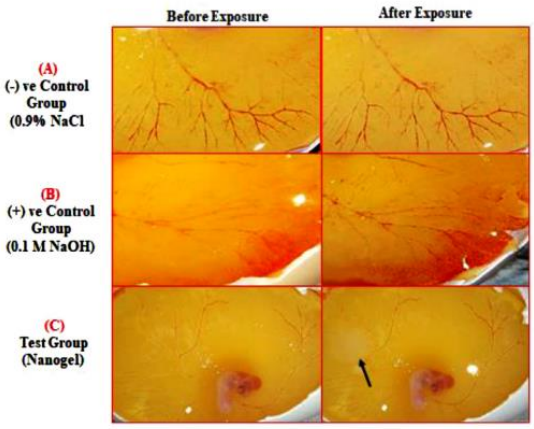

Fig. 9. Images of Het-CAM Assay captured before and after 300 seconds exposure of (A) 0.9% NaCl, (B) 0.1M NaOH (C) Griseofulvin-Loaded Nanogel (arrow).

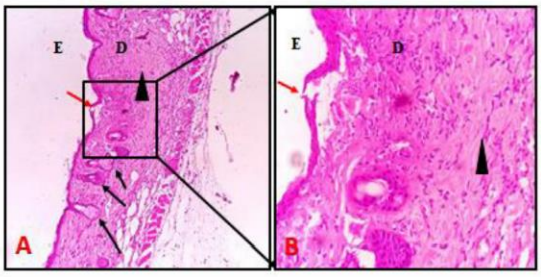

Fig. 10. Histopathology image H&E Stain at (A) 100X and (B) at 400X magnifications (Control group 1 – for Ringworm infection).

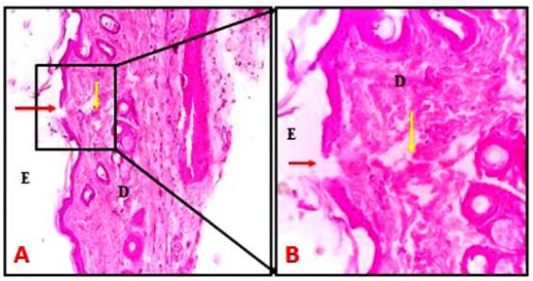

Fig. 11. Histopathology image H &E Stain at (A) 100X and (B) at 400X magnifications (Control 2 – for tenia pedis).

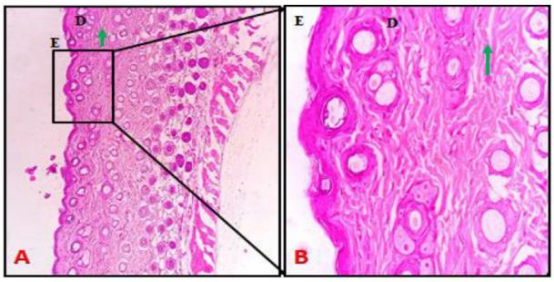

Fig. 12. (A) Histopathology image H&E Stain 100X and (B) at 400X magnifications (Test 1 – for Ringworm).

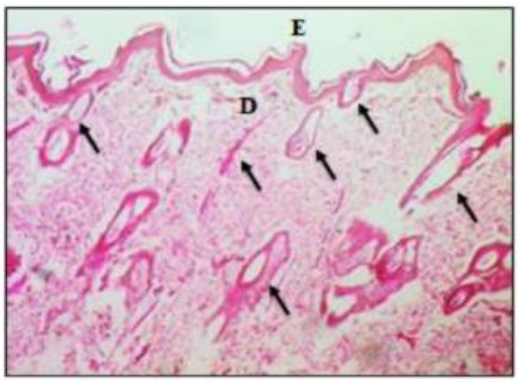

Fig. 13. Histopathology image of H&E Stain 100X (Test 2 – for tenia pedis).

3.11.2. Biochemical parameters

3.11.2.1. Lipid peroxidation.

The results of the effect of griseofulvinloaded nanogel on the lipid peroxidation are summarized in Fig 15 (For ringworm infection) and Fig 16 (For Tenia pedis infection). In group II i.e. positive control group (without treatment), the level of malondialdehyde increased significantly ($P < 0.001$) as compared to the normal control group (group I) suggesting the incidence of lipid peroxidation. There was a significant reduction ($P < 0.001$) in the lipid peroxidation noticed in groups III and IV which received griseofulvin-loaded-nanogel and marketed clotrimazole cream (standard) respectively, in comparison to positive control group animals. It was also

observed that griseofulvin loaded nanogel caused a more significant decrease in lipid peroxidation as compared to the standard drug. This suggests that the test drug was found to be more effective against lipid peroxidation as compared to the standard drug. Modification of the griseofulvin as nanogel increased the activity of the drug.

3.11.2.2. Antioxidant enzymes (Glutathione and Catalase). In the present study, a significant increase in lipid peroxidation along with a decreased level of the antioxidant enzymes, glutathione, and catalase in the positive control group was observed during the fungal infection as depicted in Fig. 16. This suggested an imbalance in peroxidant-antioxidant status and substantially the presence of oxidative stress in fungal infection. Other studies also confirmed the decreased level of glutathione and catalase during fungal infection (Indora & Kaushik, 2015, Kaur et al., 2012). The levels of reduced glutathione ($P < 0.001$) and catalase ($P < 0.01$) decreased significantly in the infected animals receiving no treatment (Group II) when compared with the normal control group (group I). Treatment with griseofulvin-loaded nanogel as well as the standard drug produced a significant increase ($P < 0.01$, $P < 0.001$) in the level of glutathione and catalase in the respective treatment groups i.e., group III and Group IV when compared with the positive control group. More significant improvement ($P < 0.001$) was shown by the group that received

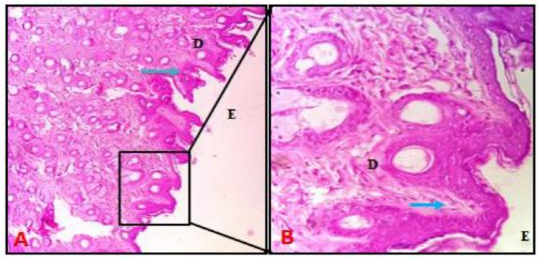

Fig. 14. (A) H&E-stained images at 100X and (B) at 400X magnification (Standard – For ringworm and tenia pedis).

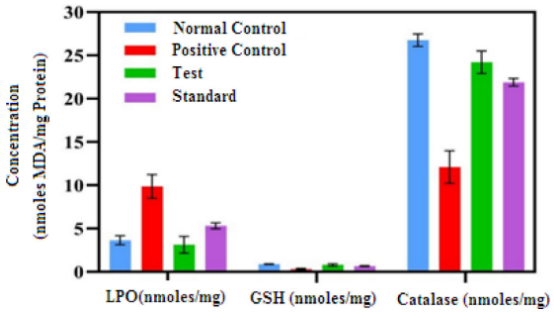

Fig. 15. Lipid peroxidation (LPO), Glutathione (GSH) and Catalase concentration in different Treatment Groups. Normal Control (I), Positive Control (II) = No treatment; Test (III) = Griseofulvin-Loaded Nanogel; Standard (VI) = (Marketed).

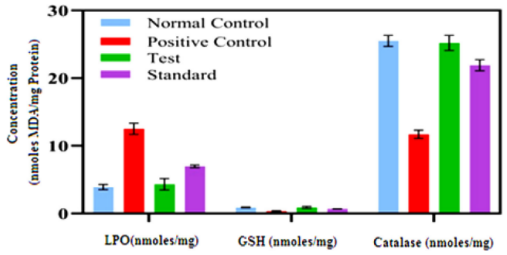

Fig. 16. Lipid peroxidation (LPO), Glutathione (GSH) and Catalase concentration in different Treatment Groups. Normal control (I) Positive Control (II) = No treatment; Test (III)=Griseofulvin-Loaded Nanogel; Standard (VI)= Griseofulvin cream (Marketed).

4. Data and statistical analysis

Data were evaluated using Turkey's test in biochemical analysis to determine the significant differences among groups. Data were expressed as mean ± standard deviation (SD). All analysis was conducted using a GraphPad Prism (Graph-Pad Software, CA, USA).

5. Conclusion

According to the study's findings, the impact of increased NLC stability on raising the ratio of liquid to solid lipid was minimal when the ratio of

Table 2 X1 = Ratio of GMS: stearic acid, X2 = Pluronic F68 & Tween 80, X3 = Sonication time (min), Y1= Particle size (nm), Y2= Entrapment efficiency (%).

Formulation code	Independent variables				Dependent variables		Zeta potential (mV)	PDI	In-vitro drug release (%)
	X1	X2	X3	X4	Y1	Y2			
F1	1:25	1.0	45	1	273±0.23	65.11±0.23	-23.6±0.22	0.177±0.23	50.12±0.32
F2	1:25	1.5	60	1.5	475.2±0.21	67.24±0.34	-29.39±0.55	0.312±0.15	55.75±0.73
F3	1:25	2.0	45	2	203.9±0.32	76.20±0.26	-27.5±0.22	0.15±0.31	75.59±0.25
F4	1:50	1.5	75	1	249.5±0.26	79.71±0.74	-24.47±0.35	0.186±0.51	67.90±0.58
F5	1:50	2.0	75	1.5	127.4±0.53	85.98±0.36	-20.86±0.27	0.092±0.13	82.11±0.63
F6	1:50	1.0	45	21	127±0.42	85.45±0.62	-28.26±0.42	0.092±0.45	82.51±0.74
F7	1:10	1.0	60	1.5	369.3±0.63	82.78±0.58	-25.3±0.56	0.252±0.33	60.12±0.52
F8	1:10	1.5	60	1	220.9±0.34	83.67±0.37	-19.7±0.32	0.247±0.32	73.67±0.38
F9	1:10	1.5	60	1.5	196.9±0.42	82.46±0.63	-24.08±0.54	0.222±0.42	76.02±0.23
F10	1:25	2.0	75	1.5	266.3±0.63	88.98±0.37	-24.08±0.42	0.292±0.53	56.34±0.26
F11	1:25	2.0	75	1	121.3±0.24	78.33±0.16	-20.61±0.24	0.089±0.25	65.12±0.35
F12	1:10	2.0	75	2	209.2±0.53	85.24±0.47	-44.12±0.52	0.237±0.43	92.24±0.13
F13	1:50	1.5	45	2	216.5±0.52	79.79±0.74	-40.38±0.35	0.249±0.52	75.24±0.35
F14	1:25	1.5	45	1.5	338.8±0.32	77.29±0.26	-33.45±0.65	0.253±0.14	68.21±0.52
F15	1:10	2.0	45	2	252.2±0.53	80.54±0.74	-55.44±0.22	0.215±0.34	76.02±0.23

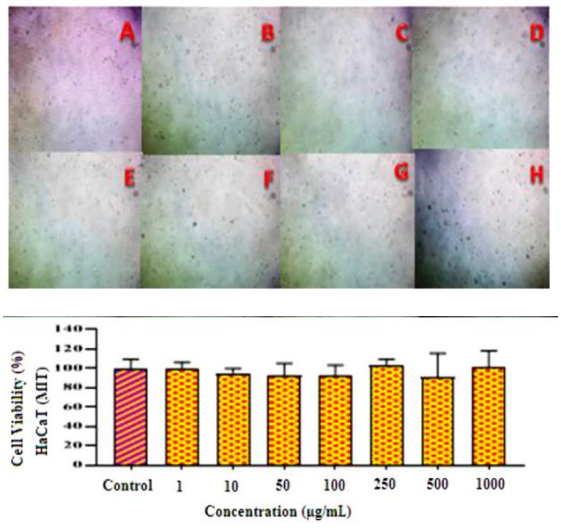

Fig. 17. HaCaT Cell Lines Control (A), HaCaT Cell Lines Treated with Different Concentrations of Griseofulvin-Loaded Nanogel (B) 1μg/mL, (C) 10 μg/mL, (D) 50 μg/mL, (E) 100 μg/mL, (F) 250 μg/mL, (G) 500 μg/mL, (H) 1000 μg/mL, and Cell Viability (%) of Griseofulvin-Loaded Nanogel on HaCaT Cells using MTT Assay (I).

Table 3 Storage stability data of optimized batch.

Storage Condition	Visual Observation	Size ± SD (nm)	PDI ± SD	Zeta Value(mV)	EE ± SD%
Room Temperature	Emulsion	112.2 ±0.141	0.183±0.008	-41.14±0.707	85±1.41
Refrigerated Condition(25^{0}c)	Emulsion	242.55±1.202	0.2635±0.303	-38.15±0.354	78.35±0.49

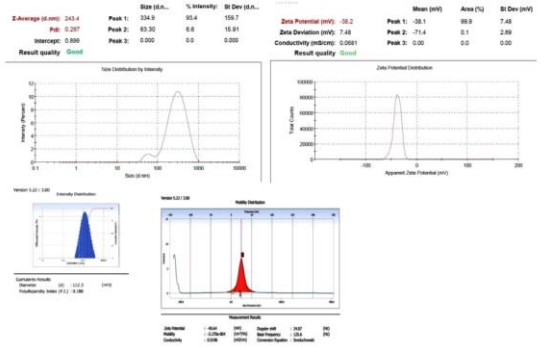

Fig. 18. Stability study of optimised batch (B12) containing Nanogel at Different temperature with respect to Particle size, PDI, Zeta potential. (n = 3, mean ± standard deviation (SD)).

There was an increase in solid lipid. Particle size and zeta potential are influenced by the duration of sonication and the proportion of liquid to solid lipids. NLCs were used in a histological investigation to reduce the infection of ringworm and tenia pedis in rat skin. After being treated with griseofulvin-loaded nanogel, the lipid peroxidation test of NLCs revealed decreased lipid peroxidation, suggesting better control of fungal infection than the commercial formulation. This could be because the level of malondialdehyde was significantly lowered. When compared to standard treatment, a group that received griseofulvin-loaded nanogel demonstrated a significant improvement, indicating that the drug's antioxidant efficacy was enhanced by the nanogel formulation, which in turn improved the drug's antifungal efficacy. According to preclinical studies, the study demonstrated

the therapeutic potential of griseofulvin-loaded nanogel for topical administration against superficial infections. It demonstrated the potential of nanogel for treating superficial infections such as ringworm and tenia pedis; as a result, it may prove to be a useful substitute for currently available treatments.

References

1. Abdel-Azeem, A. M., Salem, F. M., Mohamed, H. M., Rashad, H. M., Mohamed, R. M., & Khalil, W. F. (2012). Bioprospecting of Egyptian fungi for ecological and medical applications. In TWAS-ARO 8th Meeting (pp. 30–31). Bibliotheca Alexandrina. 10.13140/RG.2.2.21875.14882
2. Aggarwal, N., & Goindi, S. (2012). Preparation and evaluation of antifungal efficacy of griseofulvin loaded deformable membrane vesicles in optimized guinea pig model of Microsporumcanis—Dermatophytosis. International Journal of Pharmaceutics, 437(1– 3. 2), 277–287. 10.1016/j.ijpharm.2012.08.015.
3. Aggarwal, N., & Goindi, S. (2013). Dermatopharmacokinetic and pharmacodynamic evaluation of ethosomes of griseofulvin designed for dermal delivery. Journal of Nanoparticle Research, 15(10), 1–15 http://dx.doi.org/. 10.1007/s11051-013-1983-9
4. Agrawal, R., & Kaur, I. P. (2010). Inhibitory Effect of Encapsulated Curcumin on Ultraviolet-Induced Photoaging in Mice. Rejuvenation Research, 13(4), 397–410. 10.1089/rej.2009.0906.
5. Anwar, W., Dawaba, H. M., Afouna, M. I., Samy, A. M., Rashed, M. H., & Abdelaziz, A. E. (2020). Enhancing the oral bioavailability of Candesartan Cilexetil loaded nanostructured lipid carriers: In vitro characterization and absorption in rats after oral administration. Pharmaceutics, 12(11), 1047. 10.3390/pharmaceutics12111047.
6. Beg, S., Swain, S., Singh, H. P., Patra, C. N., & Rao, M. E. B. (2012). Development, optimization, and characterization of solid self-nanoemulsifying drug delivery systems of valsartan using porous carriers. AAPS PharmSciTech, 13(4), 1416–1427. 10.1208/s12249-012-9865-5.
7. Chen, Y., Zhou, L., Yuan, L., Zhang, Z., Liu, X., & Wu, Q. (2012). Formulation, characterization, and evaluation of in vitro skin permeation and in vivo pharmacodynamics of surface-charged tripterine-loaded nanostructured lipid carriers. International Journal of Nanomedicine, 7, 3023. 10.2147/ijn.s32476.
8. Cortés, H., Hernández-Parra, H., Bernal-Chávez, S. A., Prado-Audelo, M. L. D., CaballeroFlorán, I. H., Borbolla-Jiménez, F. V., González-Torres, M., Magaña, J. J., & LeyvaGómez, G. (2012). Non-ionic surfactants for stabilization of polymeric nanoparticles for biomedical uses. Materials, 14, 3197. 10.3390/ma14123197.
9. Ding, B., Zheng, Q., Yi, X., Pan, M., Chiou, Y., Yan, F., & Li, Z. (2018). Microencapsulation of sodium

bicarbonate based on glycerol monostearate and konjac glucomannan wall systems by phase separation. Food Science and Technology Research, 24(2), 249–255. 10.3136/fstr.24.249.

10. Moghddam, S. M. M., Ahad, A., Aqil, M., Imam, S. S., & Sultana, Y. (2017). Optimization of nanostructured lipid carriers for topical delivery of nimesulide using Box–Behnken design approach. Artificial Cells, Nanomedicine, and Biotechnology, 45(3), 617–624. 10.3109/21691401.2016.1167699.
11. Rouzaud, C.Olivier, C., Anabelle, B., Sylvie, F., Anne, S., Dany, A., Jean-David, B.,Nicolas, D.,Marie-Elisabeth, B., Roderick, H., Olivier, L., Fanny, L.,. (2017). Severe dermatophytosis in solid organ transplant recipients: A French retrospective series and literature review. Transplant Infectious Disease, 20(1), e12799 In press. 10.1111/tid. 12799.
12. Sandeep, D. S. (2020). Development, Characterization, and In vitro Evaluation of AceclofenacEmulgel. Asian Journal of Pharmaceutics (AJP): Free Full Text Articles from Asian J Pharm, 14(03). 10.22377/ajp.v14i03.3681.
13. Sarfraz, R. MAkram, M.R., Ali, M.R., Mahmood, A., Khan, M.U., Ahmad, H., & Qaisar, M.N. (2019). Development and In-Vitro Evaluation of pH Responsive Polymeric Nano Hydrogel Carrier System for Gastro-Protective Delivery of Naproxen Sodium. Advances in Polymer Technology, 1–13. 10.1155/2019/6090965.
14. Shimamura, T., Kubota, N., & Shibuya, K. (2012). Animal model of dermatophytosis. Journal of Biomedicine and Biotechnology, 2012, Article 125384 https://dx.doi.org/. 10.1155/2F2012/2F125384.
15. Teeranachaideekul, V., Müller, R. H., & Junyaprasert, V. B. (2007). Encapsulation of ascorbyl palmitate in nanostructured lipid carriers (NLC)—effects of formulation parameters on physicochemical stability. International Journal of Pharmaceutics, 340(1–2), 198–206. 10.1016/J.IJPHARM.2007.03.022.